relating parameter

Subscripts

TP = two phase
g = gas or vapor phase
l = liquid phase
p = pipe
ltt = liquid phase flowing alone, both phases turbulent

LITERATURE CITED

1. Bartlit, J. R., and D. K. Williamson, personal communication.
2. Förster, S., *Cryogenics*, **3**, 176 (1963).
3. Lockhart, R. W., and R. C. Martinelli, *Chem. Eng. Prog.*, **45**, 39 (1949).
4. Martinelli, R. C., L. M. K. Boelter, T. H. M. Taylor, E. G. Thomsen, and E. H. Morrin, *Trans. Am. Soc. Mech. Eng.*, **66**, 139 (1944).
5. ———, and D. B. Nelson, *ibid.*, **70**, 695 (1948).
6. Rogers, J. D., *Advan. Cryog. Eng.*, **9**, 311 (1964).
7. ———, *AIChE J.*, **14**, 895 (1968).
8. ———, and F. G. Brickwedde, *Physica*, **32**, 1001 (1966).
9. Strobridge, T. R., *Nat. Bureau Stds. Tech. Note 129* (1963).
10. Rudenko, N. S., *J. Exp. Theor. Phys.*, (*USSR*), **9**, 1078 (1939).
11. ———, and L. V. Shubnikov, *Phys. Z. Sowjetunion*, **6**, 470 (1934).
12. Wicks, M., A. E. Dukler, and R. G. Cleveland, *AIChE J.*, **10**, 38 (1964).

Axial Dispersion of Gases in Packed Beds

LESZEK Z. BALLA

Liquid Carbonic Corporation, Chicago, Illinois

and

THOMAS W. WEBER

State University of New York at Buffalo, Buffalo, New York

This study was prompted by some related work conducted here on the adsorption of gases in packed beds (*12, 16, 17*). In nearly all theoretical work on adsorption in these systems, it has been assumed that axial dispersion is small compared to bulk flow so that this dispersion could be neglected. A rather complex adsorption model was solved here using digital techniques and the results were compared with those obtained experimentally. The comparison was reasonably good, but some discrepancies were present. We felt it was desirable to measure the possible effect of axial dispersion in beds, either the same or similar to those used in the adsorption studies.

Axial dispersion in liquid systems has received considerable attention. A very comprehensive summary of this was presented by Chung and Wen (*9*). In contrast to liquid studies, relatively few have been made on gases. These are summarized in Table 1.

THEORY

Basically, two models have been used to describe the dispersion of a fluid in a packed bed, namely, the turbulent diffusive model and the mixing model. The mixing model pictures the voids of the bed as a series of well-agitated mixers as the fluid passes through. On the other hand, a perhaps more realistic picture is that the fluid particles are subjected to numerous changes in velocity, and to delays and trapping. The net result is a phenomena which may be described by a diffusional process superimposed upon a convective flow. These models have been discussed by Aris and Amundson (*2*), McHenry and Wilhelm (*15*), Levenspiel and Smith (*14*), Carberry (*6*), Carberry and Bretton (*7*), Bischoff and Levenspiel (*4*), and Sinclair and Potter (*20*). In particular, Aris and Amundson showed that for a point some distance from the bed entrance, the dispersion of a pulse by the two models would be identical.

In the present study, the diffusion model was chosen and the mathematical development and theory presented by Levenspiel (*13*), Levenspiel and Smith (*14*), and Carberry and Bretton (*7*) was followed. These treatments consider the case where a pulse of tracer is injected into a flowing stream at the entrance of the bed. The axial dispersion coefficient can then be calculated from the measured concentration at the exit. Two methods presented in these references were used for the calculation. The first involves the measured concentration corresponding to the average holdup time of the bed. The result is:

$$\left[\frac{CV_i}{Q}\right]_{\frac{vt}{V_i}=1} = \frac{1}{2\sqrt{\pi}}\left[\frac{D_L}{u_i L}\right]^{-1/2} \qquad (1)$$

Table 1. Summary of Studies of Axial Dispersion of Gases

Investigators	Gases used	Bed data	Experimental method
Deisler and Wilhelm (*10*)	H_2-N_2	column I.D. 1.1 in. ⅛ in. porous pellets	frequency response
McHenry and Wilhelm (*15*)	H_2-N_2 C_2H_4-N_2	column I.D. 1.94 in. 3 mm. glass spheres	frequency response
Carberry and Bretton (*7*)	Air-He	gas chromatographic column. 40-60 and 60-80 mesh particles.	pulse
Sinclair and Potter (*20*)	Hg. vapor-air	column I.D. 2 in. 0.0551 and 0.0172 in. glass spheres	frequency response
Chao and Hoelscher (*8*)	He-N_2	column I.D. 1 in. 0.1 in. (average) glass chips	pulse

The second method is based on calculating the variance of the experimental concentration profile at the exit. This leads to:

$$\sigma^2 = 2\frac{D_L}{u_i L} \qquad (2)$$

EXPERIMENTAL EQUIPMENT AND PROCEDURE

A diagram of the equipment is carried in Figure 1. Basically, the equipment consisted of gas-supply tanks, a pulse loop, test column, and gas analyzer. Means were also provided for controlling pressures, flow rates, and measuring the volume of gas passing through the system.

The test column was made of stainless steel tubing, 3.00 in. O.D., 2.93 in. I.D., and 5 ft. long. It was equipped with a series of sampling probes reaching to the center of the column. The first probe was located 15 in. downstream from the bed entrance and subsequent probes were spaced at 1 ft. intervals. The column was packed with solid glass spheres having a nominal diameter of 5 mm. and an average diameter of 0.016 ft. The estimated packed density of the column was 92.5 lb./cu. ft. and the void fraction was 0.365.

The flow development section ahead of the test section consisted of a 3 in. length of column packed with 5 mm. glass spheres. This section was separated from the test section by a perforated plate having 1/16 in. holes in a ¼ in. triangular pattern. No attempt was made to check the resulting velocity profile. However, Stahel and Geankoplis (*21*) state that if the ratio of the bed diameter to that of the particles is 15/1 or greater, the profile is essentially flat.

The pulse feed system included a pulse loop consisting of 8 ft. of tubing having an inside diameter of 0.152 in. and an array of five, ¼ in. quick acting Hoke toggle valves. This system, although manual, allowed for the injection of the pulse into the feed stream in a fraction of a second.

The gas analysis system consisted of the thermal conductivity cells of a Wilkens chromatograph (Model A-90-P2) connected to a recording potentiometer. The cells were of the diffusion type with large ports which made them flow sensitive but permitted fast analysis. The analysis lag due to holdup of the sampling system was minimized by using high sampling rates; this reduced the holdup time to less than a second.

Both the flow rate of gas to the column as well as the gas pressure were controlled. The flow rate of gas was found by using a dry gas meter. A wet test meter in series served as a check.

All gases were obtained from high pressure cylinders. Carrier helium gas and argon pulse gas were of standard, high purity, commercially available grade. The methane pulse gas was a special methane-helium mixture containing 17.8% methane by volume. This particular mixture was used because it was left over from some previous adsorption studies; pure methane could just as well have been used.

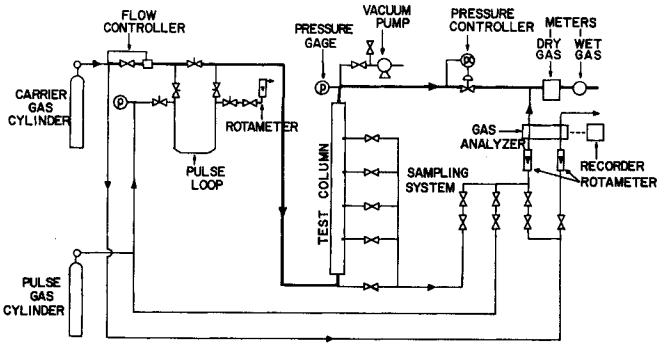

Fig. 1. Experimental flow system.

Prior to beginning a run, the system was evacuated to remove air. The pulse loop was isolated from the carrier gas system by closing the two valves at the top of the loop. Helium was then passed through the loop bypass valve, into the column, and out through the sample port to the analysis system. In the meantime, pulse gas was passed through the loop at a slow rate. The pressure was adjusted to that of the carrier gas.

Immediately before starting a test, the pulse loop was completely isolated by closing the inlet and outlet loop feed valves through which the loop gas had been passing. The carrier gas flow was then momentarily interrupted by closing the loop bypass valve and then by rapidly opening the inlet and outlet loop valves. Carrier gas was now flowing through the pulse loop pushing the pulse into the test column.

The elapsed time from the instant of pulse injection to points on the outlet pulse concentration profile was obtained from the recorder chart speed and by timing with a stopwatch.

CONDITION OF TESTS

In most of the runs, the sample tap 39 in. downstream of the entrance was used, but in a few, the first tap 15 in. from the entrance was used. Based on the estimated void fraction of the bed and the estimated volume of the feed line between the sample loop and the bed entrance, the feed line was calculated to have a holdup equivalent to 0.18 ft. of the packed bed. Hence, for the purposes of calculating times, the length of the 15 in. section was 1.43 ft. and that of the 39 in. section, 3.43 ft. The volume of the pulse loop was about 0.9% of the void volume of the 39 in. bed, making the pulse width negligible.

TABLE 2. TEST CONDITIONS AND RESULTS

Pulse : 17.8% methane — 82.2% helium

Test No.	L, ft.	Carrier gas pressure, lb./sq.in.abs.	u_i, ft./sec.	Reynolds number N_{Reei}	Reynolds number N_{Reps}	Axial dispersion coefficient, sq.ft./sec. Based on Equation (1)	Axial dispersion coefficient, sq.ft./sec. Based on Equation (2)	$(N_{Sca})^{-1}$	N_{Pea}
1	3.43	34.4	0.0118	0.128	0.130	0.000306		0.57	0.62
2	3.43	34.4	0.149	1.60	1.63	0.00126		2.34	1.88
3	3.43	34.4	0.127	1.36	1.38	0.00117		2.17	1.73
4	3.43	64.4	0.0168	0.338	0.344	0.000235		0.82	1.14
5	3.43	64.4	0.0534	1.08	1.10	0.000715		2.48	1.20
6	3.43	34.6	0.00948	0.103	0.105	0.000310	0.000300	0.56	0.50
7	3.43	34.6	0.0872	0.955	0.970	0.000772		1.43	1.80
8	3.43	98.6	0.103	3.18	3.23	0.000926	0.000950	5.06	1.73
9	3.43	98.6	0.0339	1.04	1.05	0.000330	0.000307	1.63	1.76
10	3.43	135.0	0.0814	3.48	3.53	0.000760	0.000755	5.52	1.73
11	3.43	31.9	0.0640	0.632	0.642	0.000610	0.000633	1.09	1.62
12	1.43	59.4	0.0748	1.42	1.44	0.000580	0.000570	1.87	2.10
13	1.43	59.9	0.0460	0.878	0.892	0.000431	0.000473	1.53	1.56
14	3.43	59.4	0.0745	1.38	1.40	0.000898	0.000925	2.96	1.29

All tests were made at 76°F. Gas pressures covered the range from about 34 to 135 lb./sq.in.abs. Pulse residence times ran from 19 to 473 sec.

For each run, the recorder output was converted to concentration units using a calibration made prior to the run. In all cases, the coefficient was calculated using the simplified method based on Equation (1), and in several cases, coefficients were obtained from concentration profile variances using Equation (2). Since the values obtained from spot checks based on the latter equation agreed well with those based on Equation (1), this was considered adequate and checking was limited to only a few runs.

A summary of run conditions and results for methane-helium is presented in Table 1; that for argon-helium is presented in Table 2. In addition to the axial dispersion coefficients, the calculated corresponding apparent Schmidt and Peclet numbers are presented. The word apparent is used to differentiate them from the values which would be obtained if molecular diffusivities were used. In those runs where diffusivities were calculated by the variance method, these values were used for calculating the Schmidt and Peclet numbers; in all other runs, diffusivities calculated by the simplified method were used.

CORRELATION OF RESULTS

Although only a few studies have been made of axial dispersion of gases, comparison of results is made difficult because of the variety of definitions used for the Reynolds and Peclet numbers. One of the problems with the Reynolds number is the choice of characteristic length. If an empty tube is used, then the diameter of the tube is the natural choice. However, with a packed bed, the dispersion is clearly related to particle size and this has frequently been used in calculating the Reynolds number. This basis makes comparisons with empty tube data difficult. In several studies (*4, 5, 18, 22*), an effective diameter has been used; this is somewhat analogous to the hydraulic diameter used in pipe flow:

$$d_e = \frac{4(\text{free volume of fluid})}{\text{wetted area}} = \frac{\epsilon d_t}{3/2(d_t/d_p)(1-\epsilon)+1} \quad (3)$$

When the void fraction, ϵ, is one, then $d_e = d_t$.

The problem of correlation is further magnified by the choice between using the superficial or the interstitial velocity. Thus, it's not surprising that many combinations of Reynolds and Peclet numbers have appeared. These are summarized here:

Author	Reynolds number	Peclet number
Carberry and Bretton (*7*)	$d_p u_i \rho/\mu$	$d_p u_i/D_L$
McHenry and Wilhelm (*15*)	$d_p u_s \rho/\mu$	$d_p u_i/D_L$
Sinclair and Potter (*20*)	$d_p u_s \rho/\mu$	$d_p u_s/D_L$
Chao and Hoelscher (*8*)	$d_p u_i \rho/\mu$	$d_p u_i/D_L$
This work (*3*)	$d_p u_s \rho/\mu$	$d_p u_i/D_L$
and	$d_e u_i \rho/\mu$	

The results of this study as well as those of other workers are presented in Figures 2 and 3. In Figure 2 the reciprocal of the apparent Schmidt number is correlated with the Reynolds number. The effective particle diameter was used in calculating the Reynolds number because it can be applied to both empty and packed beds. The bed parameters were such that this effective diameter is essentially the same as the particle diameter, d_p. Hence, as shown in Tables 1 and 2, Reynolds numbers calculated on either of these bases are about the same. The data of McHenry and Wilhelm (*15*), and Carberry and Bretton (*7*) are also shown as lines on the figure.

Values of molecular diffusion coefficients were estimated for each gas pair from the Gilliland Equation (11) with molecular volume data obtained from (*1*), (*11*), and (*19*). Peclet and Schmidt numbers based on these coefficients were then calculated. These limiting values are shown as dashed horizontal lines in the figure. The calculated

TABLE 3. TEST CONDITIONS AND RESULTS

Pulse : 100% argon

Test No.	L, ft.	Carrier gas pressure, lb./sq.in.abs.	u_i, ft./sec.	Reynolds number N_{Reei}	Reynolds number N_{Reps}	Axial dispersion coefficient, sq.ft./sec. Based on Equation (1)	Axial dispersion coefficient, sq.ft./sec. Based on Equation (2)	$(N_{Sca})^{-1}$	N_{Pea}
15	3.43	34.4	0.0140	0.151	0.153	0.000372		0.69	0.60
16	3.43	34.5	0.00778	0.084	0.085	0.000313		0.58	0.40
17	3.43	34.5	0.0211	0.228	0.231	0.000505	0.000490	0.91	0.69
18	3.43	36.0	0.0478	0.560	0.567	0.000873		1.69	0.88
19	3.43	36.0	0.0926	1.04	1.06	0.00134	0.00134	2.60	1.11
20	3.43	34.5	0.0418	0.452	0.458	0.000750		1.39	0.89
21	3.43	34.5	0.0107	0.113	0.115	0.000358	0.000367	0.67	0.47
22	3.43	34.5	0.0163	0.176	0.179	0.000396		0.74	0.66
23	3.43	34.5	0.0313	0.338	0.344	0.000590		1.09	0.85
24	3.43	34.5	0.0418	0.452	0.458	0.000800		1.49	0.84
25	3.43	32.3	0.00745	0.073	0.074	0.000383	0.000392	0.68	0.30

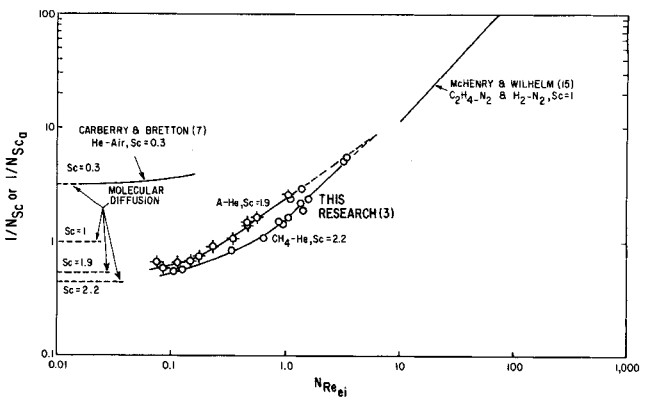

Fig. 2. Reciprocal of Schmidt number vs. Reynolds number.

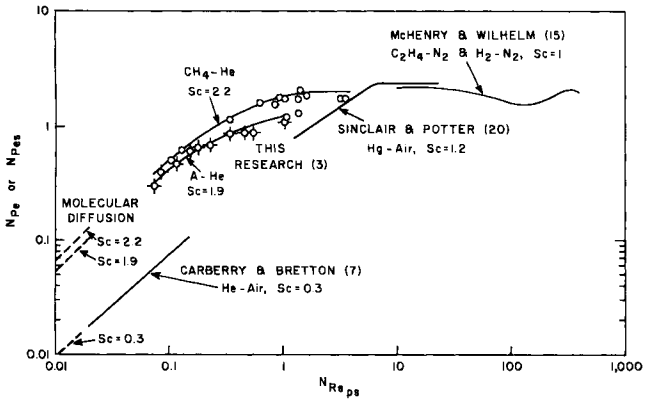

Fig. 3. Axial Peclet number vs. Reynolds number.

Schmidt numbers for the several systems are:

Gas System	Schmidt number
Methane-Helium	2.2
Argon-Helium	1.9
Helium-Air	0.3
Nitrogen-Ethylene	1.0
Mercury-Air	1.2

The data of Sinclair and Potter (*20*) and Chao and Hoelscher (8) were omitted from Figure 2 because of problems in converting their data to the correlating parameters of the graph.

In Figure 3, the Peclet number is plotted against the Reynolds number based on the particle diameter and superficial velocity. This definition was used for convenience in including the data of other studies. As is the previous figure, the lines corresponding to the limiting case of molecular diffusion are indicated.

DISCUSSION

As shown in Figures 2 and 3, the results of this study are in good agreement with those obtained by other workers. At the same time, they lie in a range of the Reynolds number where little data were previously reported.

The results, as well as those of Carberry and Bretton, indicate that at Reynolds numbers below about 0.05, the axial dispersion coefficient in a packed bed closely approaches the molecular diffusivity of the system.

In the Reynolds number range between 0.05 and 5, developing flow turbulence and eddy diffusivity gradually increase gas mixing until full turbulence is reached. In effect then, each bed void behaves as a perfect mixing cell. With increasing Reynolds number, the apparent Schmidt number tends to become independent of molecular diffusivity; this is shown in Figure 2 by the convergence of the curves for the two pairs of gases.

Peclet numbers of this study obtained at the highest Reynolds numbers appear to line up reasonably well with the limiting value of about 2. It would have been advantageous to have gone to higher Reynolds numbers. However, as the Reynolds number increases, the residence time of the gas in the bed decreases and the accuracy of the results decreases.

ACKNOWLEDGMENT

The authors wish to acknowledge the partial support of this study by The Research Foundation of the State University of New York.

NOTATION

C = tracer concentration, volume %
d_e = effective particle diameter, ft, defined by Equation (3)
d_p = particle diameter, ft.
d_t = tube or bed diameter, ft.
D_L = axial dispersion coefficient, sq.ft./sec.
D_M = molecular diffusivity, sq.ft./sec.
L = length of test section, ft.
N_{Pe} = $d_p u_i/D_M$ = Peclet number based on molecular diffusivity, particle diameter, and interstitial velocity, dimensionless
N_{Pe_a} = $d_p u_i/D_L$ = apparent axial Peclet number based on particle diameter and interstitial velocity, dimensionless
Q = volume of tracer of unit concentration which would correspond to the actual amount of tracer injected into the fluid, cu.ft.
$N_{Re_{ei}}$ = $d_e u_i \rho/\mu$ = Reynolds number based on effective particle diameter and interstitial velocity, dimensionless
$N_{Re_{ps}}$ = $d_p u_s \rho/\mu$ = Reynolds number based on particle diameter and superficial velocity, dimensionless
N_{Sc} = $\mu/\rho D_M$ = Schmidt number based on molecular diffusivity, dimensionless
N_{Sc_a} = $\mu/\rho D_L$ = apparent axial Schmidt number, dimensionless
t = time measured from the time of tracer injection into fluid, sec.
u_i = interstitial velocity of fluid, ft./sec.
u_s = superficial velocity of fluid, ft./sec.
v = volumetric flow rate of fluid, cu.ft./sec.
V_i = void volume of test section, cu.ft.
ϵ = void fraction, dimensionless
μ = bulk viscosity of fluid, lb.$_m$/ft., sec.
ρ = bulk density of fluid, lb./cu.ft.
σ^2 = variance of time-concentration curve, dimensionless

LITERATURE CITED

1. Andrussow, L., *Zeitschrift fur Phys. Chem.*, **199**, 314 (1952).
2. Aris, R., and N. R. Amundson, *AIChE J.*, **3**, 280 (1957).
3. Balla, L. Z., MS thesis, State Univer. New York, Buffalo (1968).
4. Bischoff, K. B., and O. Levenspiel, *Chem. Eng. Sci.*, **17**, 257 (1962).
5. Cairns, E. J., and J. M. Prausnitz, *ibid.*, **12**, 20 (1960).
6. Carberry, J. J., *AIChE J.*, **4**, 13M (1958).
7. ———, and R. H. Bretton, *ibid.*, **4**, 367 (1958).
8. Chao, R., and H. E. Hoelscher, *ibid.*, **12**, 271 (1966).
9. Chung, S. F., and C. Y. Wen, *AIChE J.*, **14**, 857 (1968).
10. Deisler, P. F., and R. H. Wilhelm, *Ind. Eng. Chem.*, **45**, 1219 (1953).
11. Foust, A. S., et al., "Principles of Unit Operations," John Wiley, New York (1964).
12. Lee, R. G., MS thesis, State Univer. New York, Buffalo (1967).
13. Levenspiel, O., "Chemical Reaction Engineering," John Wiley, New York (1964).
14. ———, and W. K. Smith, *Chem. Eng. Sci.*, **6**, 227 (1957).
15. McHenry, K. W., and R. H. Wilhelm, *AIChE J.*, **3**, 83 (1957).
16. Meyer, O. A., Ph.D. dissertation, State Univer. New York, Buffalo (1966).
17. ———, and T. W. Weber, *AIChE J.*, **13**, 457 (1967).
18. Mott, R. A., "Some Aspects of Fluid Flow," H. R. Lang ed., E. Arnold Publ., London (1951).
19. Perry, J. H., "Chemical Engineer's Handbook," 4th Ed., McGraw Hill, New York (1963).
20. Sinclair, R. J., and O. E. Potter, *Trans. Inst. Chem. Eng.*, **43**, T 3 (1965).
21. Stahel, E. P., and C. J. Geankoplis, *AIChE J.*, **10**, 174 (1964).
22. Wilhelm, R. H., *Chem. Eng. Prog.*, **49**, 150 (1953).